EClinicalMedicine 25 (2020) 100484

Contents lists available at ScienceDirect

EClinicalMedicine

journal homepage: https://www.journals.elsevier.com/eclinicalmedicine

Research Paper

Cerebral Micro-Structural Changes in COVID-19 Patients – An MRI-based 3-month Follow-up Study

Yiping Lu, MD[a,1], Xuanxuan Li, MD[a,1], Daoying Geng, MD, Prof[a,1], Nan Mei, MD[a,1], Pu-Yeh Wu, PhD[b], Chu-Chung Huang, PhD[c], Tianye Jia, PhD[d], Yajing Zhao, MD[a], Dongdong Wang, MD[a], Anling Xiao, MD, Prof[e,**], Bo Yin, PhD, Prof[a,*]

[a] Department of Radiology, Huashan Hospital, Fudan University, Shanghai, China (Y Lu, X Li, D Geng, N Mei, Y Zhao, D Wang, B Yin)
[b] GE Healthcare, MR Research China, Beijing, China (P Wu)
[c] Institute of Cognitive Neuroscience, School of Psychology and Cognitive Science, East China Normal University, Shanghai, China (C Huang)
[d] Institute of Psychiatry, Psychology & Neuroscience, King's College London, London, England (T Jia)
[e] Department of Radiology, Fu Yang No.2 Hospital, Anhui, China (A Xiao)

ARTICLE INFO

Article History:
Received 24 June 2020
Revised 15 July 2020
Accepted 16 July 2020
Available online 3 August 2020

Key Words:
COVID-19
Neuroimaging
Central Nervous System Diseases
Prospective studies
Diffusion Tensor Imaging

ABSTRACT

Background: Increasing evidence supported the possible neuro-invasion potential of SARS-CoV-2. However, no studies were conducted to explore the existence of the micro-structural changes in the central nervous system after infection. We aimed to identify the existence of potential brain micro-structural changes related to SARS-CoV-2.

Methods: In this prospective study, diffusion tensor imaging (DTI) and 3D high-resolution T1WI sequences were acquired in 60 recovered COVID-19 patients (56.67% male; age: 44.10 ± 16.00) and 39 age- and sex-matched non-COVID-19 controls (56.41% male; age: 45.88 ± 13.90). Registered fractional anisotropy (FA), mean diffusivity (MD), axial diffusivity (AD), and radial diffusivity (RD) were quantified for DTI, and an index score system was introduced. Regional volumes derived from Voxel-based Morphometry (VBM) and DTI metrics were compared using analysis of covariance (ANCOVA). Two sample t-test and Spearman correlation were conducted to assess the relationships among imaging indices, index scores and clinical information.

Findings: In this follow-up stage, neurological symptoms were presented in 55% COVID-19 patients. COVID-19 patients had statistically significantly higher bilateral gray matter volumes (GMV) in olfactory cortices, hippocampi, insulas, left Rolandic operculum, left Heschl's gyrus and right cingulate gyrus and a general decline of MD, AD, RD accompanied with an increase of FA in white matter, especially AD in the right CR, EC and SFF, and MD in SFF compared with non-COVID-19 volunteers (corrected p value <0.05). Global GMV, GMVs in left Rolandic operculum, right cingulate, bilateral hippocampi, left Heschl's gyrus, and Global MD of WM were found to correlate with memory loss (p value <0.05). GMVs in the right cingulate gyrus and left hippocampus were related to smell loss (p value <0.05). MD-GM score, global GMV, and GMV in right cingulate gyrus were correlated with LDH level (p value <0.05).

Interpretation: Study findings revealed possible disruption to micro-structural and functional brain integrity in the recovery stages of COVID-19, suggesting the long-term consequences of SARS-CoV-2.

Abbreviation: COVID-19, Coronavirus Disease; SARS-CoV-2, Severe Acute Respiratory Syndrome Coronavirus-2; ACE-2, Angiotensin Converting Enzyme-2; CSF, Cerebral Spinal Fluid; SARS-CoV, Severe Acute Respiratory Syndrome Coronavirus; CNS, Central Nervous System; DTI, Diffusion Tensor Imaging; TBSS, Track-based Spatial Statistics; AD, Axial Diffusivity; RD, Radial Diffusivity; MD, Mean Diffusivity; FA, Fractional Anisotropy; HIV, Human Immunodeficiency Virus; HSV, Herpes Simplex Virus; WHO, World Health Organization; PCR, Polymerase Chain Reaction; MPRAGE, Magnetization Prepared Rapid Gradient Echo; TR, Repetition Time; TE, Echo Time; FOV, Field of View; DICOM, Digital Imaging and Communications in Medicine; GMV, Gray Matter Volume; WMV, White Matter Volume; 3D-T1WI, 3 Dimensional T1-weighted Images; VBM, Voxel-based Morphometry; AAL-3, Automated Anatomical Labelling Atlas-3; WM, White Matter; GM, Gray Matter; WBC, White Blood Cell; LDH, Lactate Dehydrogenase; URTI, Upper Respiratory Tract Infection; JEV, Japanese Encephalitis Virus; UF, Uncinate Fasciculus; EC, External Capsule; CR, Corona Radiata; SFF, Superior Frontal-occipital Fasciculus; OB, Olfactory Bulb

* Correspondence to: Prof Bo Yin, Department of Radiology, Huashan Hospital, Fudan University, 12, Middle Wulumuqi Rd., Jing'an District, Shanghai 200040, China, Tel: 086-13916420317.
** Correspondence to: Prof Anling Xiao, Department of Radiology, Fuyang No.2 People`s Hospital, 450 Linquan Road, Fuyang, Anhui Province, China, Tel: 086-13053192751.
E-mail addresses: xiao2955@163.com (A. Xiao), 071105335@fudan.edu.cn (B. Yin).
[1] Contributed equally

https://doi.org/10.1016/j.eclinm.2020.100484

Funding: Shanghai Natural Science Foundation, Youth Program of National Natural Science Foundation of China, Shanghai Sailing Program, Shanghai Science and Technology Development, Shanghai Municipal Science and Technology Major Project and ZJ Lab.

Research in context

Evidence before this study

We searched PubMed and the China National Knowledge Infrastructure database for articles published up to June 10, 2020, using the keywords "COVID-19", "SARS-CoV-2", and "neurological", "DTI", and "brain". A total of 29 case reports/series reports and 106 reviews, among which 8 were systematic reviews, about the neurological findings in the central nervous system. No data has been reported about the structural changes in the brain from COVID-19 patients by functional MRI in a prospective way.

Added value of this study

In this prospective study, diffusion tensor imaging (DTI) and 3D high-resolution T1WI sequences were acquired in 60 recovered COVID-19 patients and 39 age- and sex-matched non-COVID-19 controls. We found that these recovered COVID-19 patients were more likely to have enlarged olfactory cortices, hippocampi, insulas, Heschl's gyrus, Rolandic operculum and cingulate gyrus, and a general decline of Mean Diffusivity (MD), Axial Diffusivity (AD), Radial Diffusivity (RD) accompanied with an increase of Fractional Anisotropy (FA) in white matter, especially AD in the right Coronal Radiata (CR), External Capsule (EC) and Superior Frontal-occipital Fasciculus (SFF), and MD in SFF compared with non-COVID-19 volunteers. Global Gray Matter Volume (GMV), GMVs in left Rolandic operculum, right cingulate, bilateral hippocampi, left Heschl's gyrus, and Global MD of WM were found to correlate with memory loss. GMVs in right cingulate gyrus and left hippocampus were related to smell loss. MD-GM score, global GMV, and GMV in right cingulate gyrus were correlated with Lactate Dehydrogenase (LDH) level.

Implications of all the available evidence

Our findings revealed possible disruption to micro-structural and functional brain integrity in the recovery stages of COVID-19, suggesting neuro-invasion potential of SARS-CoV-2. This requires attention since even if the patients recover well from the pneumonia condition, the neurological changes may cause a great burden. More research in the mechanism and route of neuro-invasion of SARS-CoV-2 is expected.

1. Introduction

Coronavirus Disease 2019 (COVID-19), an illness caused by the novel Severe Acute Respiratory Syndrome Coronavirus-2 (SARS-CoV-2), is an on-going viral pandemic and has spread to the whole world. To date, it has been spreading globally with nearly 4,700,000 active infections and the total death toll was over 560,000 [1]. As a member of the coronavirus family, SARS-CoV-2 shares a 77.2% amino acid identity, 72.8% sequence identity and structural similarity with Severe Acute Respiratory Syndrome Coronavirus (SARS-CoV) [2,3]. With high affinity of the receptor-binding domain of Angiotensin Converting Enzyme-2 (ACE-2), SARS-CoV-2 invades human cells in the same way as SARS-CoV [4,5]. In light of the neurological invasion of SARS-CoV proved by abundant studies, it is plausible to hypothesize that SARS-CoV-2 has the potential to attack the central nervous system (CNS) as well [6].

Increasing evidence supported the neuro-invading potential of SARS-CoV-2. According to the first-hand evidence from Wuhan, 36.4% of COVID-19 patients presented neurological symptoms such as dizziness, headache and impaired consciousness during hospitalization. Furthermore, the percentage and extensiveness were higher in severe patients [7]. Except the frequent olfactory and gustatory dysfunctions in mild-to-moderate COVID-19 patients recorded by 12 European hospitals, scattered cases of various neurological diseases including encephalitis, stroke, micro-hemorrhage, hemorrhage posterior reversible encephalopathy and cerebral venous embolism were also reported in hospitalized patients [8–10]. Additionally, it was documented that the specific SARS-CoV-2 RNA was detected in the cerebral-spinal fluid (CSF) of a COVID-19 patient [11]. Although no definite description of the pathological findings has been recorded, all the aforementioned evidence indicated SARS-CoV-2 was neuro-invasive just like SARS-CoV [12].

Based on previous researches, coronaviruses can cause demyelination, neurodegeneration, and cellular senescence which accelerate brain aging and exacerbate neurodegenerative pathology [4,13–16]. However, only scattered neurological cases in COVID-19 patients were collected to document the neurological changes during the acute infection period and so far, no long-term observation has been conducted to explore possible structural changes in the CNS. Despite satisfactory recovery in the majority of COVID-19 patients, they will have a great burden if there are neurological consequences. Therefore, it was necessary to investigate the long-term impact of SARS-CoV-2 infection on the CNS, especially on the structures easily attacked by virus and the structures highly-expressing ACE-2 [3,17].

In contrast to the pathological methods, in-vivo Magnetic Resonance Imaging (MRI) could reflect the cerebral structures non-invasively. The possible micro-structural damage in CNS could be detected by structural MRI and diffusion tensor imaging (DTI). Axial diffusivity (AD), radial diffusivity (RD), mean diffusivity (MD) and fractional anisotropy (FA) can be calculated using track-based spatial statistics (TBSS) [18]. Together with volumetric analysis, DTI is widely used in a large scale of neuro-radiological studies to detect micro-structural changes in patients with cerebral viral infections, Human Immunodeficiency Virus (HIV) and Herpes Simplex Virus (HSV), etc [19,20]. So far, no researches have been found to describe the cerebral changes after SARS-CoV-2 infection.

Therefore, in the current study, we aimed to apply volumetric and diffusion measurements in recovered COVID-19 patients to identify the existence of potential long-term brain structural changes related to SARS-CoV-2, which could provide better insights to understand the impact of SARS-CoV-2 on the CNS.

2. Material and Methods

This was a prospective study, which was approved by the local ethics committee (No.20200616017) and written informed consent was obtained from each participant.

2.1. Participant Cohort

We planned to enroll 155 consecutive recovered COVID-19 patients who were discharged from Fuyang No.2 People`s Hospital (the only designated hospital for infectious diseases in Fuyang, Anhui Province) to take MRI and clinical follow-up. The criteria of diagnosis and discharge of COVID-19 patients were based on the Polymerase Chain Reaction (PCR) result according to World Health Organization (WHO) guidelines [21]. The non-COVID-19 volunteers were recruited through social media. Each volunteer agreed to take the MRI scan and finished a questionnaire. Finally, 60 COVID-19 patients and 39 age- and sex-matched non-COVID-19 volunteers were successfully recruited to undertake three-dimensional T1-weighted imaging (3D-T1WI) and DTI scans. No artefacts were observed in their MR images.

2.2. Clinical assessment

The clinical characteristics of COVID-19 patients were obtained from the hospital records including age, gender, clinical type (mild/severe/critical type, according to WHO guidelines [21]), hospitalization days, existence of fever, cough, gastrointestinal symptoms, known contact history, alcohol intake history, smoking history and laboratory tests including white blood cell (WBC) count, lymphocyte count and lactate dehydrogenase (LDH). The laboratory tests were done at admission.

A semi-quantitative scoring system (CT extent score) was used to estimate the severity of pneumonia by assessing the CT scan at admission [22]. Each lung was divided into upper (above the tracheal carina), lower (below the inferior pulmonary vein) and middle (in between) zones, and each zone was scored based on the following criteria: 0, 0%; 1, $<$ 25%;2, 25% - 49%; 3, 50% - 74%; 4, $>$ 75%. The abnormal extent was determined by the summation of scores (possible range 0-24).

The detailed neurological symptoms both during infection and at this follow-up visit were collected via self-report, including the existence of headache, vision changes, hearing loss, loss of smell, loss of taste, impaired mobility, limb numbness, tremor, fatigue, myalgia, memory loss, mood changes. Handedness was also included in the questionnaire.

For non-COVID-19 volunteers, the basic information about age, gender, handedness, alcohol intake history, smoking history and underlying diseases were recorded.

2.3. Neuroimaging

Neuroimaging was performed using a 3.0 T Magnetom Skyra (Siemens, Germany). The structural 3 Dimensional T1-weighted Images (3D-T1WI) were acquired in sagittal plane using T1-weighted 3D Magnetization Prepared Rapid Gradient Echo (MPRAGE) sequence, with parameter setting: TR/TE=1900/2.84 ms, flip angle=5°, acquisition matrix=256 $\times$ 256, FOV=280 $\times$ 280 mm^2, number of slices=160 and slice thickness=0.9mm.

DTI sequence was twice-refocused spin-echo sequence based on single-shot echo-planar acquisition. Diffusion sensitizing gradients were applied along 90 orthogonal directions using two b values (0 and 1000 s/mm^2) and other DTI parameters were: TR=3700 ms, TE=92 ms, FOV=220 $\times$ 220 mm^2, matrix=128 $\times$ 128 and slice thickness=4.0 mm (voxel size 1.7 $\times$ 1.7 $\times$ 4.0 mm). The acquisition time per dataset was approximately 10 minutes. The original raw data were anonymized and transferred from the scanner in the DICOM format.

2.4. Voxel-based Morphometry (VBM) and Atlas-based Analysis

To calculate the quantitative parameters including gray matter volume (GMV), white matter volume (WMV), FA, MD, RD and AD values of different brain regions, we followed an atlas-based image processing approach (Figure 1). DTI datasets were first processed using DSI Studio software (http://dsi-studio.labsolver.org/) to generate FA, MD, RD and AD maps for each subject. Second, we performed a rigid

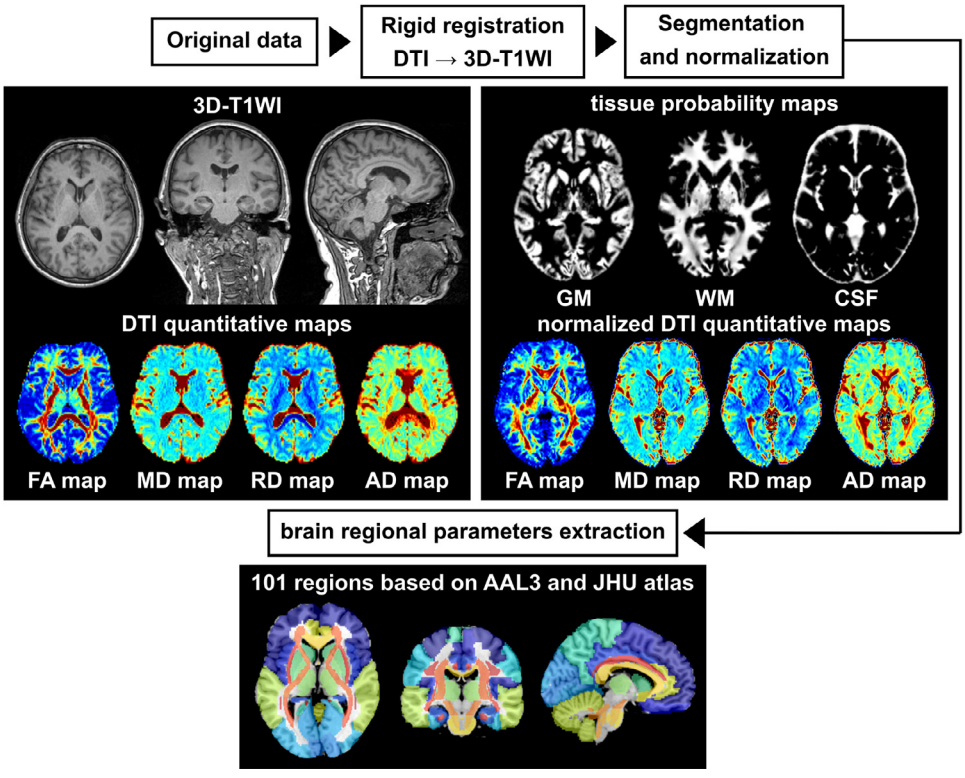

Figure 1. The atlas-based imaging processing workflow

registration between the DTI quantitative maps and 3D-T1WIs using SPM12 software (http://www.fil.ion.ucl.ac.uk/spm/) based on MATLAB (MathWorks, Natick, MA, USA). Third, 3D-T1WIs were segmented and nonlinearly normalized into MNI space using CAT12 toolbox (http://www.neuro.uni-jena.de/cat/) implemented in SPM12 to get the tissue probability maps and normalized DTI quantitative maps. Fourth, we combined the automated anatomical labelling atlas-3 (AAL-3) [23] and JHU DTI-based White Matter (WM) atlas [24] for quantitative parameters extraction in GM and WM, respectively. Finally, the brain was parcellated into 65 (AAL-3) plus 36 (JHU DTI-based WM atlas) anatomical regions. Brain regional volumes, and diffusion indices including FA, MD, RD and AD of WM and GM respectively can be extracted by averaging the values from voxels with partial volume exceeding 90% of the corresponding tissue. The estimated global GMV and WMV were further normalized by correction of intracranial volume.

2.5. Stratification

We stratified our findings based on the following rules in order to further investigate the impact of the factors of interest on the global or regional volumetric or diffusive indices that were significantly different between groups. 1) Handedness: The data was compared between righthanded and lefthanded patients. 2) Neurological symptoms during acute stage: The data was compared between patients with and without neurological symptoms during acute stage. 3) Neurological symptoms at follow-up point: The data was compared between patients with and without neurological symptoms at the follow-up point. 4) Clinical severity. We allocated mild patients into non-severe subgroup, and severe subgroup included severe and critical ones and explored the difference.

2.6. Abnormality assessment

We used a semi-quantitative scoring system by respectively comparing regional MD values of GM and WM, and FA values of WM between patients and controls: 0 not involved, MD GM or MD WM value in the patient is within 1 standard deviations (SD) of that in controls; 1 positive mild alteration, the value in the patient is 1 SD above but within 2 SD of that in controls; -1 negative mild alteration, the value in the patient is -1 SD below but within -2 SD of that in controls; 2 positive clear alteration, the value in the patient is 2 SD above that in controls; -2 negative clear alteration, the value in the patient is -2 SD below that in controls. The total index scores were calculated as a sum of the score (named MD-GM score) in each of the 65 brain regions according to AAL atlas, and in each of the 36 regions according to JHU atlas (named MD-WM and FA-WM scores). The MD-GM score ranged from -130 to 130 and the MD-WM and FA-WM scores ranged from -72 to 72 [25].

2.7. Correlation analysis

The assessment of the correlation was performed among different index scores, regional volumes and diffusion indices with significant inter-group differences, and clinical characteristics.

2.8. Statistical Analysis

All statistical analyses were performed with R software (version 3.5.3; R Foundation for Statistical Computing, Vienna, Austria). The Shapiro-Wilk test and Levene's test was used to evaluate the distribution type and homogeneity of variance. Volumetric and diffusion indices were compared between COVID-19 and control groups using analysis of covariance (ANCOVA) to adjust the effects of age, gender and whole brain volume. To control for multiple comparisons in brain regional analysis, false discovery rate (FDR) method was applied to correct the p value. Two sample t-test and Chi-squared test/ Fisher exact test were performed to compare the continuous and categorical measurements between two groups. Spearman Correlation coefficients were calculated to explore relationship between volumetric/ diffusion indices and clinical data. A p value of <0.05 was defined as statistical significance.

3. Role of Funding

No study sponsor had any role in study design; collection, analysis, or interpretation of data; or in writing this paper or the decision to submit for publication. The corresponding author had full access to all study data and had final responsibility for the decision to submit for publication.

4. Results

4.1. Baseline

We recruited 60 COVID-19 patients (mean age ± SD, 44.10 ± 16.00 years; Male: 34/60, 56.70%) into the COVID-19 group and another 39 age- and sex-matched non-COVID-19 volunteers (mean age ± SD, 45.88 ± 13.90 years; Male: 22/39, 56.40%) were enrolled as the control group. COVID-19 patients were all diagnosed and hospitalized in January and February, and the MRI scans were done in May (mean duration from the onset to the date of MRI scans, 97.46±8.01 days). During SARS-CoV-2 infection, 41/60 (68.33%) patients had neurological symptoms including mood change (25, 41.67%), fatigue (16, 26.67%), headache (15, 25.00%), vision change (13, 21.67%), myalgia (9, 15.00%), impaired mobility (7, 11.67%), memory loss (8, 13.33%), taste loss (4, 6.67%), limb numbness (4, 6.67%), tremor (4, 6.67%), smell loss (2, 3.33%) and hearing loss(1, 1.67%). Other common symptoms included fever (53/60, 88.33%), cough (34/60, 56.67%), and gastrointestinal discomfort (8/60, 13.33%). At this follow-up visit, 33/60 (55%) patients still had neurological symptoms. The numbers of patients feeling fatigue and mood change declined significantly compared with before (p value < 0.05). 47 (78.33%) of the patients were classified as the mild type of COVID-19, 12 (20.00%) patients were severe type, and 1 (1.67%) was grouped as critical type. (Table 1)

4.2. Voxel-based Morphometry (VBM)

The comparisons of the mean regional GMVs between the COVID-19 group and the control group were reported in Table 2 and those of WMVs were shown in Table 3. VBM analysis showed the significantly higher GMV in the left Rolandic operculum area (p value = 0.019), bilateral olfactory cortices (p value = 0.024 and 0.043 for left and right), bilateral insulas (p value = 0.013 and 0.013), bilateral hippocampi (p value < 0.001, and = 0.013), right cingulate gyrus (p value = 0.118) and left Heschl's gyrus (p value < 0.001) in COVID-19 patients. No significant differences were seen in other regional GMVs or any regional WMVs (all p values > 0.05).

4.3. Diffusion Indices

The comparisons of diffusion indices were performed. Differences in regional MD values of gray matter between two groups were collected in Table 4, and regional FA, MD, AD and RD values of white matter were illustrated in Table 5. In the gray matter of COVID-19 patients, the left insula (p value <0.001), bilateral cingulate gyri (p value = 0.039 and 0.305), right precuneus (p value = 0.279), and right thalamus (p value = 0.033) were found to have significantly lower MD values when compared with the control group. In white matter, the mean regional MD, AD and RD values were generally lower in the COVID-19 group, and the mean regional FA values were generally higher compared with the controls. The mean MD values of right

Table 1
Baseline information of the COVID-19 group and the control group

	Control Group (n=39)	COVID-19 Group (n = 60)		*P* value
Age, Mean±SD	45.88±13.90	44.10±16.00		0.558
Gender, male(%)	22 (56.41%)	34 (56.67%)		0.980
Known contact history, n(%)	0 (0.00%)	33 (55.00%)		<0.001*
Alcohol, n(%)	11 (28.21%)	19 (31.67%)		0.834
Smoking, n(%)	10 (25.64%)	15 (25.00%)		1
Underlying diseases, n(%)				
Hypertension	16 (41.03%)	13 (21.67%)		0.142
Diabetes	1 (2.56%)	6 (10.00%)		0.250
Clinical type, n(%)				
Mild type	-	47 (78.33%)		-
Severe type	-	12 (20.00%)		-
Critical type	-	1 (1.67%)		-
Hospitalization days, Mean±SD	-	15.35±6.05		-
Symptoms, n(%)				
Fever	-	53 (88.33%)		-
Cough	-	34 (56.67%)		
Gastrointestinal	-	8 (13.33%)		-
Neurological	-	**During acute stage**	**At follow-up visit point**	
Total*		41 (68.33%)	33 (55.00%)	0.032
Headache	-	15(25.00%)	6 (10.00%)	0.055
Vision change	-	3 (5.00%)	1 (1.67%)	0.619
Hearing loss	-	1 (1.67%)	1 (1.67%)	1
Loss of taste	-	4 (6.67%)	1 (1.67%)	0.364
Loss of smell	-	2 (3.33%)	2 (3.33%)	1
Impaired mobility	-	7 (11.67%)	4 (6.67%)	0.529
Numbness in extremities	-	4 (6.67%)	4 (6.67%)	1
Tremor	-	4 (6.67%)	1 (1.67%)	0.364
Fatigue	-	16 (26.67%)	4 (6.67%)	0.006*
Myalgia	-	9 (15.00%)	15 (25.00%)	0.254
Memory loss	-	8 (13.33%)	17 (28.33%)	0.071
Mood change	-	25 (41.67%)	10 (16.67%)	0.005*
Laboratory tests, median (interquartile range)				
WBC count, *10^9/L	-	4.7 (3.85-6.76)		-
Lymphocyte count, *10^9/L	-	1.06 (0.77-1.49)		-
LDH, U/L	-	223 (189.5-279.5)		-
Treatment				
Oxygen therapy		37 (61.67%)		
Anti-viral therapy		58 (96.67%)		
Interferon		9 (15.00%)		
Antibiotics		21 (35.00%)		
Hormonotherapy		2		

Abbreviations: SD: Standard Deviation; WBC: White Blood Cell; LDH: Lactate Dehydrogenase.
* **Total count and percentage of patients that presented any of the following neurological symptoms during the acute stage and at the follow-up visit point respectively. One patient possibly had one or more types of symptoms.**

superior frontal-occipital fasciculus (SFF) (p value = 0.036) in the COVID-19 group, and the AD values in right corona radiata (CR) (p value <0.001), right external capsule (EC) (p value = 0.048) and right SFF (p value <0.001) of COVID-19 group were significantly lower than the control group. No significant differences were found in regional FA or RD values (all p values>0.05).

4.4. Global Analysis

The differences in global GMV along with diffusion indices of white matter, the AD, RD, MD, and the FA were summarized in Table 6. Significantly higher mean global GMV (F = 143, p value= 0.02), higher global FA value (F = 100, p value = 0.021), lower global MD (F = 80, p value= 0.001), AD (F = 87, p value= 0.002) and RD (F = 72, p value= 0.002) were found in the COVID-19 group than the control group.

The regions with significant differences in the volumes and diffusion indices between these two groups were shown in Figure 2.

4.5. Stratification

The results were collected in Supplementary Table 1. No statistically significant differences were found in the indices of interest between patients that were righthanded (n = 54) and lefthanded (n=6), patients with (n = 41) and without (n = 19) neurological symptoms during acute stage, patients with (n = 33) and without (n = 27) neurological symptoms at the follow-up point, or patients classified as non-severe (n = 47) and severe (n = 13) (all p values> 0.05). Additionally, we were interested in the changes of regions in the olfactory cortex-related regions in patients with smell loss, thus related regional GMVs and MD of GM were compared (Supplementary Table 2). No significant differences were found in either comparison (all p values > 0.05), yet the average regional GMVs and MD of GM of patients with smell loss (n = 2) were generally lower than patients without the symptom (n = 58).

4.6. Index scores

Three index scores, namely FA-WM, MD-GM, and MD-WM scores of each COVID-19 patient were calculated and compared between the patients and the controls. No statistically significant differences were found between the mean index scores (COVID-19 VS control, FA-WM: 0.050 VS -1.359, p value = 0.371; MD-GM: 0.750 VS 1.769, p value = 0.282; MD-WM: 0.167 VS 1.333, p value = 0.951).

The assessment of the correlation was performed among different index scores, regional volumes (including global GMV and 9 regional

Table 2
Comparison of regional GMV between the control group and COVID-19 group

Region (cm^3)	Left				Right			
	Control (n=39)	COVID-19 (n=60)	F	*p* value	Control (n=39)	COVID-19 (n=60)	F	*P* value
Precentral	8.34	8.53	51	0.343	7.58	7.76	48	0.390
Frontal	43.58	45.18	167	0.053	43.64	45.17	157	0.070
Rolandic*	3.11	3.34	193	0.019*	3.90	4.12	136	0.094
Supp_Motor	5.30	5.44	50	0.379	6.10	6.23	40	0.463
Olfactory*	1.29	1.37	182	0.024*	1.18	1.25	174	0.043*
Rectus	2.82	2.93	116	0.121	2.69	2.81	140	0.080
OFC	6.00	6.19	121	0.118	5.60	5.78	96	0.144
Insula*	7.20	7.60	54	0.013*	6.98	7.38	55	0.013*
Cingulate*	7.78	8.05	123	0.118	7.20	7.56	189	0.019*
Hippocampus*	3.94	4.20	61	<0.001*	3.45	3.67	58	0.013*
ParaHippocampal	2.88	2.93	49	0.390	4.08	4.20	83	0.226
Amygdala	1.10	1.15	141	0.080	1.01	1.03	39	0.463
Calcarine	6.58	6.66	18	0.827	5.18	5.16	6	0.972
Cuneus	4.20	4.21	7	0.972	3.87	3.85	9	0.966
Lingual	6.50	6.59	27	0.618	6.90	6.96	15	0.827
Occipital	15.39	15.78	70	0.302	11.47	11.54	12	0.849
Fusiform	9.32	9.66	122	0.118	9.66	9.95	97	0.144
Postcentral	9.63	9.71	16	0.827	9.18	9.17	3	0.972
Parietal	13.04	13.15	19	0.800	8.23	8.22	5	0.972
SupraMarginal	3.89	4.02	68	0.321	5.51	5.52	4	0.972
Angular	3.96	4.08	72	0.293	4.74	4.86	45	0.414
Precuneus	9.50	9.72	52	0.331	9.36	9.46	21	0.699
Paracentral Lobule	2.84	2.94	47	0.390	2.00	2.02	14	0.832
Caudate	2.53	2.65	71	0.296	2.71	2.73	13	0.832
Putamen	3.63	3.70	20	0.712	2.99	2.99	4	0.972
Pallidum	0.20	0.20	8	0.972	0.46	0.45	10	0.920
Thalamus	3.58	3.68	34	0.544	3.87	3.98	35	0.520
Heschl*	0.64	0.71	64	<0.001*	0.73	0.78	142	0.080
Temporal	41.31	42.74	151	0.074	41.33	42.10	65	0.323
Cerebelum	37.53	37.51	2	0.981	36.45	36.64	11	0.920
Vermis (bilateral)	5.99	5.90	24	0.673	4.47	4.70	148	0.074
ACC	4.47	4.70	148	0.074	3.85	3.94	33	0.544
NAC	0.63	0.66	163	0.053	0.64	0.66	69	0.321

Supp_Motor: Supplementary Motor Area; OFC: Orbital Frontal Cortex; ACC: Anterior Cingulate & Paracingulate Gyri; NAC: Nucleus Accumbens.
P values were corrected by means of false discovery rate (FDR).
* Corrected p value < 0.05.

Table 3
Comparison of regional WMV between the control group and COVID-19 group

Region (cm^3)	Left				Right			
	Control (n=39)	COVID19 (n=60)	F	*p* value	Control (n=39)	COVID19 (n=60)	F	*P* value
MCP (bilateral)	10.97	11.51	111	0.144	10.97	11.51	111	0.144
PCT (bilateral)	1.14	1.17	68	0.510	1.14	1.17	68	0.510
CC (bilateral)	23.27	23.17	7	0.947	23.27	23.17	7	0.947
Fornix (bilateral)	0.30	0.30	4	0.956	0.30	0.30	4	0.956
CST	1.05	1.08	98	0.456	1.05	1.07	42	0.599
ML	0.52	0.53	65	0.510	0.51	0.52	56	0.510
ICP	0.69	0.72	100	0.456	0.70	0.72	86	0.456
SCP	0.54	0.55	80	0.507	0.53	0.54	52	0.554
CP	1.61	1.65	97	0.456	1.60	1.61	26	0.779
IC	6.09	6.23	81	0.507	6.31	6.36	18	0.812
CR	12.97	13.25	71	0.510	13.02	13.30	57	0.510
PTR	2.87	2.87	3	0.958	3.04	3.02	8	0.924
SS	1.61	1.65	83	0.456	1.69	1.72	53	0.554
EC	3.03	3.12	58	0.510	2.96	3.03	47	0.554
Cingulate	1.91	1.91	5	0.947	1.60	1.59	5	0.947
Hippocampus	0.73	0.72	24	0.799	0.81	0.80	30	0.701
SLF	4.99	4.98	2	0.987	5.08	5.10	6	0.947
SFF	0.30	0.31	85	0.456	0.30	0.30	45	0.568
UF	0.21	0.20	46	0.557	0.23	0.22	15	0.820
Tapetum	0.14	0.15	99	0.456	0.19	0.20	84	0.456

Abbreviations: MCP: Middle Cerebellar Peduncle; PCT: Pontine Crossing Tract; CC: Corpus Callosum; CST: Corticospinal Tract; ML: Medial Lemniscus; ICP: Inferior Crebellar Peduncle; SCP: Superior Cerebellar Peduncle; CP: Cerebral Peduncle; IC: Internal Capsule; CR: Corona Radiata; PTR: Posterior Thalamic Radiation; SS: Sagittal Stratum; EC: External Capsule; SLF: Superior Longitudinal Fasciculus; SFF: Superior Fronto-occipital Fasciculus; UF: Uncinate Fasciculus.
P values were corrected by means of false discovery rate (FDR).

Table 4
Comparison of regional MD of GM between the control group and COVID-19 group

Region ($10^{-3}mm^2/s$)	Left				Right			
	Control (n=39)	COVID-19 (n=60)	F	*p* value	Control (n=39)	COVID-19 (n=60)	F	*P* value
Precentral	0.91	0.91	2	0.952	1.06	1.10	141	0.366
Frontal	0.93	0.91	26	0.527	1.02	1.04	13	0.623
Rolandic	1.14	1.09	164	0.085	0.98	0.96	153	0.246
Supp_Motor	0.96	0.99	140	0.374	0.81	0.82	49	0.500
Olfactory	0.94	0.93	14	0.615	0.88	0.86	137	0.402
Rectus	0.93	0.91	16	0.537	0.85	0.83	116	0.466
OFC	0.92	0.92	6	0.931	0.92	0.89	142	0.346
Insula*	0.88	0.84	154	<0.001*	1.03	1.01	149	0.305
Cingulate*	0.93	0.90	172	0.039*	0.83	0.79	144	0.033*
Hippocampus	0.95	0.96	8	0.823	1.02	1.01	10	0.710
ParaHippocampal	1.01	0.97	148	0.346	0.93	0.93	4	0.931
Amygdala	0.85	0.83	136	0.402	0.88	0.89	12	0.709
Calcarine	1.00	0.99	11	0.710	0.95	0.94	110	0.466
Cuneus	1.05	1.04	15	0.605	0.92	0.89	167	0.072
Lingual	1.03	1.00	155	0.219	0.95	0.92	165	0.076
Occipital	0.92	0.92	3	0.952	0.90	0.88	157	0.215
Fusiform	0.96	0.94	147	0.346	0.92	0.90	158	0.209
Postcentral	1.03	1.05	22	0.527	1.08	1.10	20	0.528
Parietal	1.02	1.02	7	0.931	1.14	1.16	27	0.527
SupraMarginal	0.92	0.89	170	0.072	1.01	1.01	5	0.931
Angular	0.94	0.94	9	0.823	0.97	0.93	169	0.072
Precuneus*	1.11	1.08	151	0.279	0.90	0.86	145	<0.001*
Paracentral Lobule	1.06	1.09	143	0.346	0.88	0.86	98	0.467
Caudate	0.99	0.94	159	0.209	0.99	0.92	163	0.116
Putamen	0.72	0.70	166	0.076	0.77	0.72	162	0.130
Pallidum	0.68	0.65	135	0.415	0.76	0.73	132	0.439
Thalamus*	0.92	0.89	146	0.346	0.79	0.75	173	0.033*
Heschl	0.95	0.95	3	0.952	1.20	1.12	168	0.072
Temporal	0.89	0.86	171	0.054	0.94	0.92	138	0.402
Cerebelum	0.84	0.83	120	0.466	0.85	0.83	134	0.415
Vermis (bilateral)	0.94	0.91	150	0.305	0.94	0.91	150	0.305
ACC	0.94	0.91	139	0.380	0.82	0.80	156	0.219
NAC	0.91	0.82	161	0.184	0.85	0.78	160	0.184

Supp_Motor: Supplementary Motor Area; OFC: Orbital Frontal Cortex; ACC: Anterior Cingulate & Paracingulate Gyri; NAC: Nucleus Accumbens.
P values were corrected by means of false discovery rate (FDR).
* Corrected p value < 0.05.

Table 5
Differences in regional diffusion indices of white matter between COVID-19 group and control group

	Region ($10^{-3}mm^2/s$)	Left				Right			
		Control (n=39)	COVID-19 (n=60)	F	*p* value	Control (n=39)	COVID-19 (n=60)	F	*P* value
FA	-	-	-	-	-	-	-	-	-
MD	SFF	-	-	-	-	0.75	0.677	81	0.036*
AD	CR	-	-	-	-	1.117	1.076	88	<0.001*
	EC	-	-	-	-	1.121	1.091	106	0.048*
	SFF	-	-	-	-	1.125	1.04	95	<0.001*
RD	-	-	-	-	-	-	-	-	-

FA: Factional Anisotropy; MD: Mean Diffusivity; AD: Axial Diffusivity; RD: Radial Diffusivity; CR: Corona Radiata; EC: External Capsule; SFF: Superior Fronto-occipital Fasciculus.
P values were corrected by means of false discovery rate (FDR).
* Corrected p value < 0.05.

Table 6
Global mean gray matter volume and various white matter diffusion indices in the control group and COVID-19 group.

Area	Control Group (n=39)	COVID-19 Group (n = 60)	F	*P* value
GMV **(cm^3)**	585.848	598.987	143	0.02*
FA **($10^{-3}mm^2/s$)**	0.389	0.404	100	0.021*
MD **($10^{-3}mm^2/s$)**	0.784	0.759	80	0.001*
RD **($10^{-3}mm^2/s$)**	0.611	0.582	72	0.002*
AD **($10^{-3}mm^2/s$)**	1.132	1.113	87	0.002*

GMV: Gray Matter Volume; FA: Factional Anisotropy; MD: Mean Diffusivity; AD: Axial Diffusivity; RD: Radial Diffusivity.
* Corrected p value < 0.05.

GMVs) and diffusion indices (including 4 global indices of WM, 1 regional MD of WM, 5 regional MD of GM, and 3 regional AD of WM) with significant inter-group differences, and clinical characteristics.

1) Correlation with neurological symptoms during acute stage

The significant correlations were shown in Figure 3 and Supplementary Table 3 between neurological symptoms during the acute stage and regional WMVs, diffusion indices, and index scores. MD values of GM in right thalamus and AD values of WM in right EC were positively correlated with vision changes (r = 0.336 and 0.285 respectively, p value = 0.027 and 0.046 respectively). GMVs in right cingulate and hippocampus were negatively correlated with smell loss

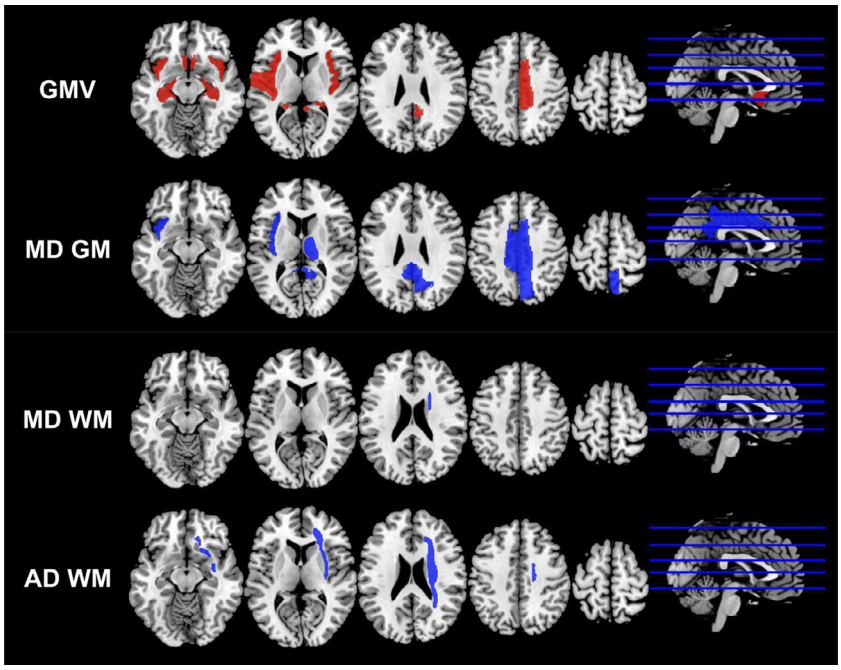

Figure 2. The regions with statistically significant differences in the volumes and diffusion indices of the COVID-19 group compared with the control group. The regions with relative higher mean values in the COVID-19 group were marked as red, and the regions with relative lower mean values in the COVID-19 group were marked as blue. GMV: gray matter volume; MD GM: mean diffusivity of gray matter; MD WM: mean diffusivity of white matter; AD WM: axial diffusivity of white matter.

(r = -0.284 and -0.279 respectively, *p* value = 0.028 and 0.031 respectively).

2) Correlation with neurological symptoms at this follow-up visit

The correlations were also shown in Figure 3 and Supplementary Table 3. FA-WM score was negatively related to tremor (r = -0.262, *p* value = 0.043), and MD-WM score was positively correlated (r = 0.279, *p* value =0.031). Global GMV and regional GMV in left Rolandic operculum, right cingulate, bilateral hippocampus, and the left Heschl's gyrus, as well as global MD value of WM were all negatively correlated with memory loss (r = -0.341, -0.369, -0.394, -0.321, -0.277, -0.279 and -0.285 respectively, *p* value = 0.008, 0.002, 0.009, 0.012, 0.032, 0.031, 0.027). MD values of GM in cingulate gyri were correlated with fatigue (r = 0.305 and 0.320, *p* value =0.018 and 0.013 respectively for the left and the right) and numbness in the extremities (r = 0.286, *p* value = 0.027), and MD of GM in right precuneus correlated to numbness (r = 0.309, *p* value = 0.016). Figure 3 displayed all the correlation (*p* value < 0.01).

3) Correlation with other important clinical data

Other important clinical data included handedness, typing of COVID-19, CT extent score, etc. MDs of GM in bilateral cingulate gyri were found to correlate with clinical type (*p* value = 0.035 and 0.036 for left and right side). Other significant correlations can be found in Figure 4 and Supplementary Table 4.

4) Correlation with Laboratory results

MD-GM score (r = -0.317, *p* value = 0.014), global GMV (r = -0.282, *p* value = 0.029), and GMV in right cingulate gyrus (r =0.160, *p* value = 0.041) correlated with LDH. A variety of indices were found to correlate with WBC count and lymphocyte percentage. (See Figure 4 and Supplementary Table 4). A plot with regression was produced for the correlation between LDH and global GMV (Figure 5).

5. Discussion

In this prospective work, we recorded the detailed cerebral volumetric, DTI metrics 3 months after SARS-CoV-2 infection by applying DTI and 3D T1WI in 60 recovered COVID-19 patients and 39 age- and sex-matched normal volunteers. Overall, these recovered COVID-19 patients were more likely to have enlarged olfactory cortices, hippocampi, insulas, Heschl's gyrus, Rolandic operculum and cingulate gyrus, and a general decline of MD, AD, RD accompanied with an increase of FA in white matter, especially AD in the right CR, EC and SFF, and MD in SFF compared with non-COVID-19 volunteers. Global GMV, GMVs in left Rolandic operculum, right cingulate, bilateral hippocampus, left Heschl's gyrus, and Global MD of WM were found to correlate with memory loss. GMVs in right cingulate gyrus and left hippocampus were related to smell loss. MD-GM score, global GMV, and GMV in right cingulate gyrus were correlated with LDH level.

Given the olfactory and gustatory dysfunction in COVID-19 patients and evidence of olfactory epithelium invasion by SARS-CoV, the olfactory gyrus was thought to be the first functional area in CNS to be infected by SARS-CoV-2 [26]. To avoid cross-infection, patients were unable to undertake MRI scans during the acute phase, but we are still curious about whether any micro-structural changes exist in the recovery stage of COVID-19 and whether any clues were left to suggest the probable intracranial infection route.

According to our results, significant enlarged volumes were observed in the bilateral olfactory cortices, hippocampi, insulas, left Heschl's gyrus, left Rolandic operculum and right cingulate gyrus. All these structures mentioned above belonged to the central olfactory system. Among them, olfactory cortex, also named as piriform cortex, directly receives axonal projections from olfactory bulb (OB), is referred to as a part of 'primary olfactory cortex'. Other structures are the cortical targets of primary olfactory cortex in the bilateral limbic lobe, temporal cortices, which were referred as 'secondary olfactory cortex' [27]. It was reported that the frequent olfactory loss during the course of upper respiratory tract infections (URTI) resulted in loss of stimulation and subsequent volume loss in the acute phase, while after olfactory recovery, the volumes of GM in the central olfactory

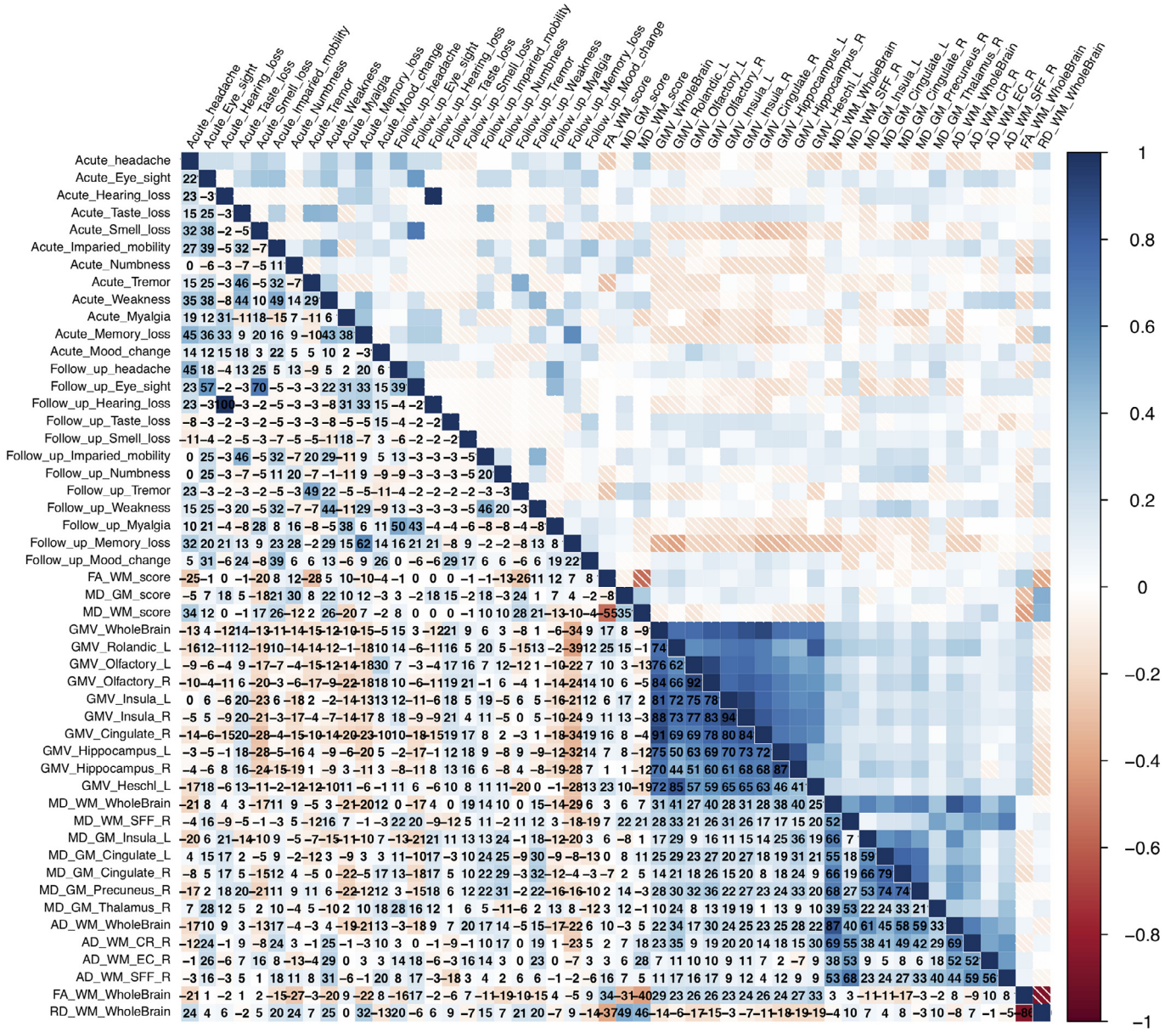

Figure 3. Correlation among brain scores, regional volumes and diffusion indices with neurological symptoms during acute stage. The range of correlation coeffcients (CCs) is between -1 to 1. The numbers in the figure are CCs * 100 for the convenience of display. Abbreviations: GMV: Gray Matter Volume; WMV: White Matter Volume; GM: Gray Matter; WM: White Matter; FA: Factional Anisotropy; MD: Mean Diffusivity; AD: Axial Diffusivity; RD: Radial Diffusivity; CR: Corona Radiata; EC: External Capsule; NAC: Nucleus Accumbens; L: Left; R: Right.

system got enlarged subsequently [28,29]. We analyzed the GMV difference between patients with or without olfactory loss and found the GMVs of the central olfactory system were generally smaller in patients with persistent olfactory loss compared with those without olfactory problems which was aligned with previous similar studies (**Supplementary Table 2**) [28].

Several possible invasion routes of SARS-CoV-2 were raised including hematogenous, lymphatic and neuro retrograde routes, etc., yet the exact route was unknown. Based on our findings, the gray matter volumetric changes in the central olfactory system provided a speculation that SARS-CoV-2 might enter the CNS via an OB-mediated neuronal retrograde route. Two reasons were suspected to play a role in these GMV enlargement: the neurogenesis and functional compensation. Firstly, patients were suspected to experience neurogenesis. It is well accepted that neurogenesis in adults are restricted to two regions, the subventricular zone (SVZ) and the subgranular layer of the dentate gyrus of the hippocampus [30]. The neuroblasts from SVZ migrate along the rostral migratory stream, enter olfactory cortex first and finally replace interneurons (e.g., periglomerular cells, granular cells) in the OB [30]. Therefore, the increasing neurons possibly resulted in the enlargement of the GMV in the olfactory system. Secondly, in order to compensate for impaired olfaction, the increased functional engagement of brain regions would be hypertrophy, which was proved to have enlarged neurons and increasing number of dendritic spines by experimental studies in sensory deprivation models [28]. These two reasons might be an explanation of the enlarged GMV, while further pathological exploration was needed.

In general, lower diffusivity parameters (MD, AD, RD) and higher FA values were recognized in the white matter from COVID-19 cohort. In addition, the diffusivity (MD and AD) of right CR, EC and SFF decreased significantly. The CR, consisting massive bundle of

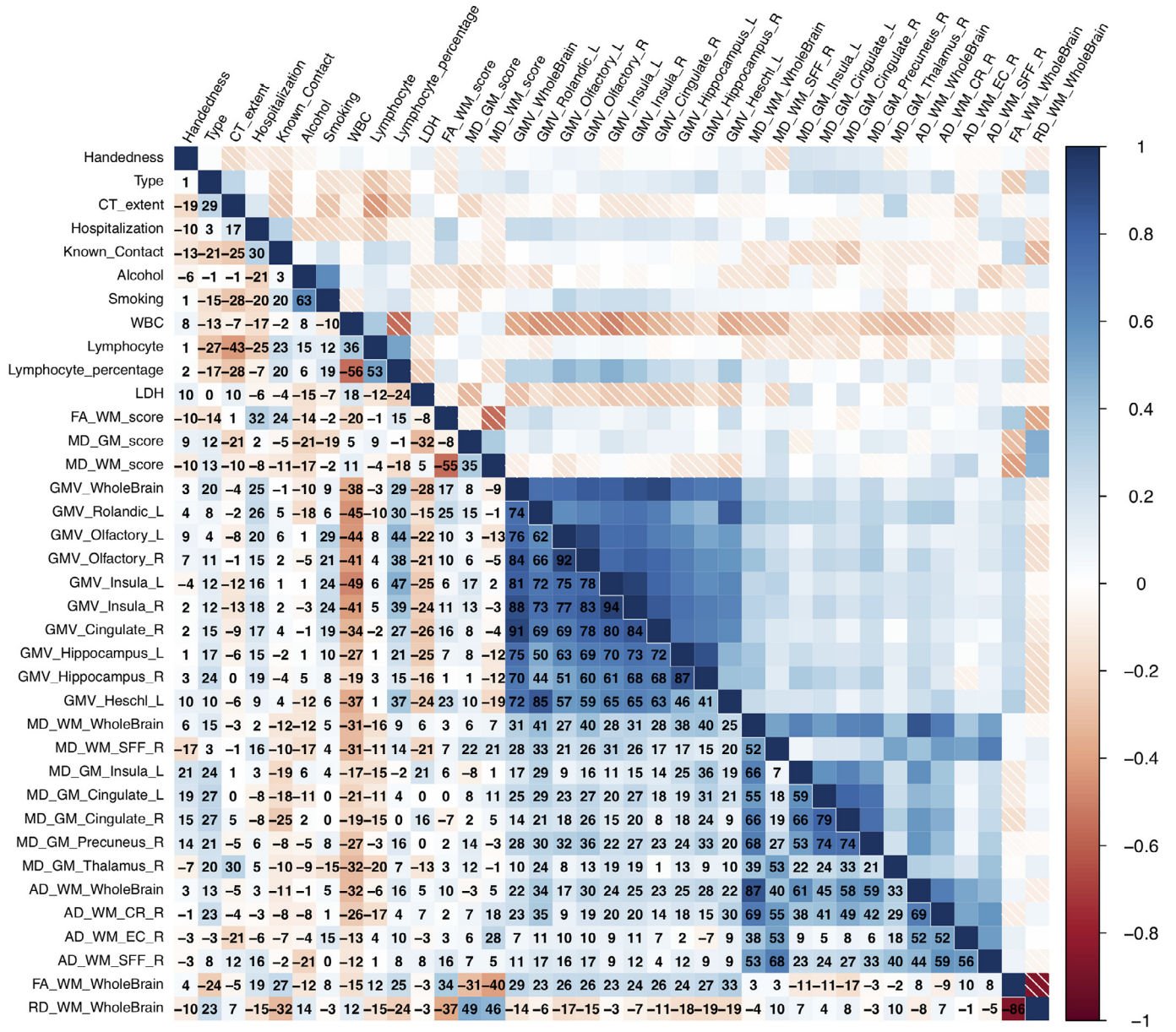

Figure 4. Correlation among brain scores, regional volumes and diffusion indices with neurological symptoms at follow-up visit. The range of correlation coeffcients (CCs) is between -1 to 1. The numbers in the figure are CCs * 100 for the convenience of display. Abbreviations: GMV: Gray Matter Volume; WMV: White Matter Volume; GM: Gray Matter; WM: White Matter; FA: Factional Anisotropy; MD: Mean Diffusivity; AD: Axial Diffusivity; RD: Radial Diffusivity; CR: Corona Radiata; EC: External Capsule; NAC: Nucleus Accumbens; L: Left; R: Right.

projection fibers, connects the cortex to the brainstem and the thalamus in afferent and efferent manners [31]. The EC and SFF are series of association fibers, connecting frontal, parietal, and temporal cortices. White matter was not the main target for neurotropic virus; however, the connecting fibers could act as the channel for intracranial viral transmission. Different from the elevated MD with compressed volume in fibers in hydrocephalus, the enlargement of white matter fibers, decreased MD values and elevated FA suggested a greater alignment of fibers and limited diffusion freedom, indicating a possible intrinsic re-construction (e.g. remyelination) process that occurred after infection [32].

It was interesting to notice that all the diffusivity abnormalities in the white matter restricted in the right hemisphere, without asymmetrical symptoms reported by COVID-19 patients. Since the blood flow rate and volume was higher in the hemisphere dominant for handedness, we hypothesized that the predominance of abnormal white matter diffusivities might be related to the difference of blood volume in bilateral hemispheres [33]. However, after comparing these abnormal diffusivity indices between lefthanded and right-handed patients, no difference was found (Supplementary Table 1). The asymmetrical phenomenon was detected in other studies as well [28,34]. The right-side predominance in odorant perception has been indicated by multiple olfactory functional studies which was not fully understood. The diffusivity changes on the right side might be related to the right-side odorant perception in which further exploration was needed [28].

During SARS-CoV-2 infection, 41/60 (68.33%) patients had neurological symptoms and over 50% recovered patients still had symptoms 3 months later. It was interesting to find the GMV in hippocampi (a key part in the organization of memory) and cingulate gyri (an important part of limbic system) were negatively related to loss of smell during infection and loss of memory 3 month later,

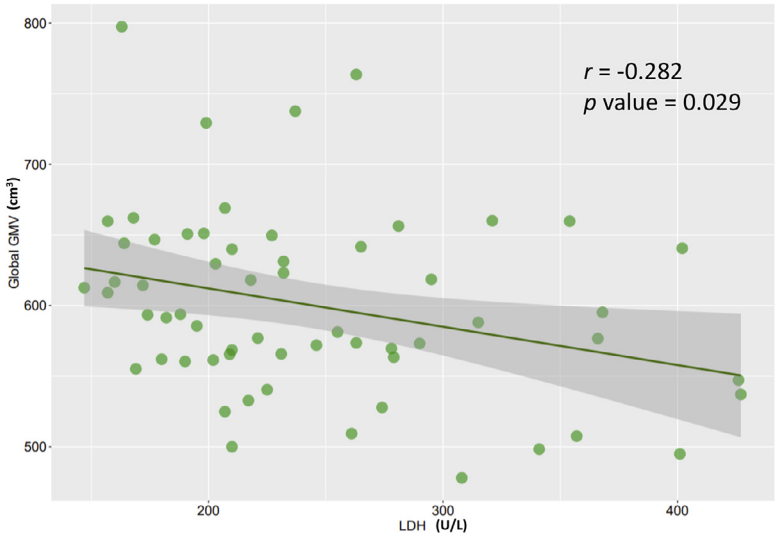

Figure 5. A scatter plot with regression was produced for the correlation between LDH (U/L) and global GMV (cm^3). LDH: Lactate Dehydrogenase; GMV: Gray Matter Volume

which could support our hypothesis of neurogenesis in these regions mentioned above. Tremor was found to be negatively related to FA_WM score both in the acute stage and at the 3-month follow-up point which indicated a destruction of WM fibers in both hemispheres, possibly resulted from SARS-CoV-2 induced cytokine storm [35].

According to WHO guideline, COVID-19 patients were divided into mild, severe and critical types based on their clinical information and laboratory results [21]. No significant difference was observed between severe and non-severe groups. But the clinical types were positively related to MD values in bilateral cingulate gyri (r=0.271 and 0.272, p=0.035 and 0.036 respectively), implying the more severe the case was, the higher the MD value of bilateral cingulate gyri was presented. Cingulate gyrus usually plays an important role in attention, motivation, decision making, learning, and cost-benefit calculation, as well as conflict and error monitoring, which is frequently affected in limbic encephalitis [36]. Therefore, the dysregulated cytokine response was speculated in severe cases [35].

After exploring the relationship between laboratory data and DTI metrics, the global GMV was significantly but slightly correlated with the LDH concentration in COVID-19 patients. LDH is one of the key enzymes in the glycolytic pathway, highly expressed in cells from kidney, heart, liver and brain [37]. Elevated concentrations of LDH are observed in patients with encephalitis, ischemic stroke and head injuries [37]. Higher concentration of serum LDH always follows tissue breakdown and is closely linked to the deterioration and poor outcome [38]. The decreased global GMV in LDH-elevated patients might indicate an atrophy due to a severe inflammatory response.

Since the hemostatic abnormalities, including disseminated intravascular coagulation (DIC) and severe inflammatory response, were frequently observed in COVID-19 patients, individuals may predispose to cerebral-vascular events caused by infection and treatment [39]. An index score system was introduced into our study to investigate the existence of micro-structural abnormalities due to microvessel diseases. The ischemic changes are known to be accompanied with lower FA value and higher MD value in the ischemic lesions. However, our findings showed that FA-WM score was higher, MD-GM and MD-WM scores were lower in the COVID-19 group compared with the control group, and the differences were insignificant. Thus, no obvious evidence of micro-vessel diseases was found.

It is important to investigate the relationship between abnormal anatomical brain areas and ACE-2 distribution. It is clarified that SARS-CoV-2 enters the host cell by attaching with ACE-2 via Spike (S) glycoprotein. Therefore, the more expression of ACE-2 might bring more severe abnormalities. The distribution of ACE2 was non-equivalent over the brain and was most frequently expressed in substantia nigra, followed by spinal cord, hippocampus, basal ganglia, limbic system and frontal cortex [17]. Our results suggested that various components in the limbic system were affected structures sharing possible high ACE-2 expression, which were partly aligned with the proposed ACE-2-riched regions. Although we were not able to observe the DTI metrics in substantia nigra since it was not included in the brain atlas we used, it was still very hard to support any relationship between ACE2 expression and affected brain areas.

At the time of writing, there was still no research to detect the cerebral micro-structural changes after SARS-CoV-2 infection from imaging or pathological aspects. Our study gave a hint to possible neurological changes after SARS-CoV-2 infection. The limitations of our study were listed as follows: 1) we did not enroll enough patients with neurological dysfunction or olfactory loss, therefore the relationship between GMV/diffusivity changes and olfactory symptoms would be missed; 2) as a single-centered study, a selection bias might result from limited ethnical and regional characteristics of the participants, and possible mutants of SARS-CoV-2 in other countries, and limit the generalization of the study; 3) the atlas we applied did not contain the structure in brainstem, therefore, we failed to obtain the volumetric and DTI information about the nucleus in brainstem, some of which were quite important, especially the solitary nuclei.

In this prospective study, volumetric and micro-structural abnormalities were detected mainly in the central olfactory cortices, partial white matter in the right hemisphere from recovered COVID-19 patients, providing new evidence to the neurological damage of SARS-CoV-2. The abnormalities in these brain areas might cause long-term burden to COVID-19 patients after recovery, which was thus worth public attention.

6. Contributors

Yiping Lu, Bo Yin and Daoying Geng conceived and designed the research. Yiping Lu, Anling Xiao, Xuanxuan Li, Nan Mei, Yajing Zhao and Dongdong Wang contributed to data collection and interpretation. Yiping Lu, Xuanxuan Li, Pu-Yeh Wu, Chu-Chung Huang and Tianye Jia contributed to statistical analysis. Yiping Lu, Xuanxuan Li and Nan Mei contributed to draft and revise the manuscript. Anling Xiao

and Bo Yin supervised the whole research. Yiping Lu, Xuanxuan Li, Daoying Geng and Nan Mei contributed equally to this study. All authors gave final approval for the version to be published.

Data Sharing Statement

According to the informed consent, all the data involved is only used in this research and our institution. Thus, supporting data is not available for the public due to the ethical restriction.

Declaration of interests

The authors declare that they have no known competing financial interests or personal relationships that could have appeared to influence the work reported in this paper. This paper has never been published elsewhere.

Acknowledgments

We thank Wei Cheng (Ph.D., Institute of Science and Technology for Brain-Inspired Intelligence, Fudan University) for providing statistical consultation and technological support.

Funding

This project was supported by Shanghai Natural Science Foundation (Grant No. 18ZR1405700), Youth Program of National Natural Science Foundation of China (Fund No. 81901697), Shanghai Sailing Program (Grant No. 18YF1403000), Shanghai Science and Technology Development (Fund No. 19511121204), Shanghai Municipal Science and Technology Major Project (No. 2018SHZDZX01) and ZJ Lab. All the funding sources played no roles in the study.

Supplementary materials

Supplementary material associated with this article can be found in the online version at doi:10.1016/j.eclinm.2020.100484.

References

[1] Coronavirus Cases. Available online:https://www.worldometers.info/coronavirus/(accessed on 18 June 2020). 2020.
[2] Wu F, Zhao S, Yu B, et al. A new coronavirus associated with human respiratory disease in China. Nature 2020;579:265–9.
[3] Brielle ES, Schneidman-Duhovny D, Linial M. The SARS-CoV-2 exerts a distinctive strategy for interacting with the ACE2 human receptor. Viruses 2020;12. doi: 10.3390/v12050497.
[4] Desforges M, Le Coupanec A, Stodola JK, Meessen-Pinard M, Talbot PJ. Human coronaviruses: Viral and cellular factors involved in neuroinvasiveness and neuropathogenesis. Virus Res 2014;194:145–58.
[5] Hamming I, Timens W, Bulthuis MLC, Lely AT, Navis GJ, van Goor H. Tissue distribution of ACE2 protein, the functional receptor for SARS coronavirus. A first step in understanding SARS pathogenesis. J Pathol 2004;203:631–7.
[6] Xu J, Zhong S, Liu J, et al. Detection of Severe Acute Respiratory Syndrome Coronavirus in the Brain: Potential Role of the Chemokine Mig in Pathogenesis. Clin Infect Dis 2005;41:1089–96.
[7] Mao L, Wang M, Chen S, et al. Neurologic Manifestations of Hospitalized Patients With Coronavirus Disease 2019 in Wuhan, China. JAMA Neurol 2020 **Epub ahead**: E1–8.
[8] Baig AM. Updates on What ACS Reported: Emerging Evidences of COVID-19 with Nervous System Involvement. ACS Chem Neurosci 2020;11:1204–5.
[9] Poillon G, Obadia M, Perrin M, Savatovsky J, Lecler A. Cerebral Venous Thrombosis associated with COVID-19 infection: causality or coincidence? J Neuroradiol 2020. doi: 10.1016/j.neurad.2020.05.003.
[10] Hanna Huang Y, Jiang D, Huang JT. A Case of COVID-19 Encephalitis. 2020 DOI:10.1016/j.bbi.2020.05.012.
[11] Moriguchi T, Harii N, Goto J, et al. A first case of meningitis/encephalitis associated with SARS-Coronavirus-2. Int J Infect Dis 2020;94:55–8.
[12] Xu Z, Shi L, Wang Y, et al. Pathological findings of COVID-19 associated with acute respiratory distress syndrome. Lancet Respir Med 2020;8:420–2.
[13] Lane TE, Hosking MP. The pathogenesis of murine coronavirus infection of the central nervous system. Crit Rev Immunol 2010;30:119–30.
[14] Baz-Martínez M, Da Silva-Álvarez S, Rodríguez E, et al. Cell senescence is an antiviral defense mechanism. Sci Rep 2016;6:1–11.
[15] Hascup ER, Hascup KN. Does SARS-CoV-2 infection cause chronic neurological complications? GeroScience 2020. doi: 10.1007/s11357-020-00207-y.
[16] Jasti M, Nalleballe K, Dandu V, Onteddu S. A review of pathophysiology and neuropsychiatric manifestations of COVID-19. J Neurol 2020. doi: 10.1007/s00415-020-09950-w.
[17] Chen R, Wang K, Yu J, Chen Z, Wen C, Xu Z. The spatial and cell-type distribution of SARS-CoV-2 receptor ACE2 in human and mouse brain. *bioRxiv*2020;: 2020.04.07.030650.
[18] Maximov II, Thönneßen H, Konrad K, Amort L, Neuner I, Shah NJ. Statistical Instability of TBSS Analysis Based on DTI Fitting Algorithm. J Neuroimaging 2015;25:883–91.
[19] Ragin AB, Wu Y, Gao Y, et al. Brain alterations within the first 100 days of HIV infection. Ann Clin Transl Neurol 2015;2:12–21.
[20] Bradshaw MJ, Venkatesan A. Herpes Simplex Virus-1 Encephalitis in Adults: Pathophysiology, Diagnosis, and Management. Neurotherapeutics 2016;13:493–508.
[21] World Healthy Organization. Clinical management of severe acute respiratory infection when COVID-19 is suspected (v1.2). Who; 2020. p. 1–21.
[22] Zheng Y, Xiao A, Yu X, et al. Development and Validation of a Prognostic Nomogram Based on Clinical and CT Features for Adverse Outcome Prediction in Patients with COVID-19. Korean J Radiol 2020;21:1–11.
[23] Rolls ET, Huang CC, Lin CP, Feng J, Joliot M. Automated anatomical labelling atlas 3. Neuroimage 2020;206:116189.
[24] Hua K, Zhang J, Wakana S, et al. Tract probability maps in stereotaxic spaces: Analyses of white matter anatomy and tract-specific quantification. Neuroimage 2008;39:336–47.
[25] Eisenmenger L, Porter M, Carswell C, Mead S, Rudge P, Collinge J. Diffusion-weighted MRI signal abnormality in sporadic CJD increases in extent and intensity with disease duration. JAMA Neurol 2018;73:76–84.
[26] Netland J, Meyerholz DK, Moore S, Cassell M, Perlman S. Severe Acute Respiratory Syndrome Coronavirus Infection Causes Neuronal Death in the Absence of Encephalitis in Mice Transgenic for Human ACE2. J Virol 2008;82:7264–75.
[27] Han P, Zang Y, Akshita J, Hummel T. Magnetic Resonance Imaging of Human Olfactory Dysfunction. Brain Topogr 2019;32:987–97.
[28] Karstensen HG, Vestergaard M, Baaré WFC, et al. Congenital olfactory impairment is linked to cortical changes in prefrontal and limbic brain regions. Brain Imaging Behav 2018;12:1569–82.
[29] Gellrich J, Han P, Manesse C, et al. Brain volume changes in hyposmic patients before and after olfactory training. Laryngoscope 2018;128:1531–6.
[30] Curtis MA, Kam M, Nannmark U, et al. Human neuroblasts migrate to the olfactory bulb via a lateral ventricular extension. Science 2007;315:1243–9 *(80-)*.
[31] Yakar F, Eroglu U, Peker E, Armagan E, Comert A, Caglar H. Structure of corona radiata and tapetum fibers in ventricular surgery. J Clin Neurosci 2018. doi: 10.1016/j.jocn.2018.08.041.
[32] Cauley KA, Cataltepe O. Axial diffusivity of the corona radiata correlated with ventricular size in adult hydrocephalus. Am J Roentgenol 2014;203:170–9.
[33] Jansen van Vuuren A, Saling MM, Ameen O, Naidoo N, Solms M. Hand preference is selectively related to common and internal carotid arterial asymmetry. Laterality 2017;22:377–98.
[34] Bitter T, Gudziol H, Burmeister HP, Mentzel HJ, Guntinas-Lichius O, Gaser C. Anosmia leads to a loss of gray matter in cortical brain areas. Chem Senses 2010;35:407–15.
[35] Mehta P, McAuley DF, Brown M, Sanchez E, Tattersall RS, Manson JJ. COVID-19: consider cytokine storm syndromes and immunosuppression. Lancet 2020;395:1033–4.
[36] Ibi K, Fujii K, Kobayashi H, Senda M, Kitazawa K, Honda A. Anterior cingulate cortex involvement in non-paraneoplastic limbic encephalitis. Brain Dev 2019;41:735–9.
[37] Valvona CJ, Fillmore HL, Nunn PB, Pilkington GJ. The Regulation and Function of Lactate Dehydrogenase A: Therapeutic Potential in Brain Tumor. Brain Pathol 2016;26:3–17.
[38] Augoff K, Hryniewicz-Jankowska A, Tabola R. Lactate dehydrogenase 5: An old friend and a new hope in the war on cancer. Cancer Lett 2015;358:1–7.
[39] Bikdeli B, Madhavanj M V, Jimenez D, et al. COVID-19 and Thrombotic or Thromboembolic Disease: Implications for Prevention, Antithrombotic Therapy, and Follow-up. J Am Coll Cardiol 2020 https://doi.org/10.1016/j.jacc.2020.04.031.